244 *Bull. Korean Chem. Soc., Vol. 9, No. 4, 1988*

Hyun Woo Cho et al.

Physical Adsorption of Nitrogen Gas on BN, Alumina, and Silica-Gel Powders

Hyun-Woo Cho, Jung-Soo Kim⁺, Eun-Ah Yoo⁺, and Woon-Sun Ahn*

Department of Chemistry, Sung Kyun Kwan University, Suwon 440-746
⁺Department of Chemistry, Sung Shin Women's University, Seoul 136-742
Received March 25, 1988

Multilayer adsorption isotherms of nitrogen on hexagonal boron nitride, γ-alumina, and silica-gel powders are determined at the liquid nitrogen temperature using a gravimetric adsorption apparatus. The volume (V) of the adsorbed gas are plotted against the statistical thickness(t) of the adsorbed layer, and the t-method area are calculated from the slope of these V-t plots to compare with the BET area. A number of universal adsorption isotherms and the Frenkel-Halsey-Hill equation are used one after another in calculating the statistical thickness. The appropriateness of the FHH equation as an universal adsorption isotherm is discussed finally.

Introduction

The multilayer physisorption isotherm of nitrogen gas on the high energy surfaces, such as silica and alumina surfaces, is of great importance, and many theoretical and empirical adsorption isotherms have been proposed.[1] The experimental verification or the generalization of these isotherms are almost impossible, while each of the isotherms has some advantage over the others. The development of numerous sophisticated surface studying instruments, such as LEED, AES, and various electron spectrometers, enabled the study of adsorption on well-defined single crystal surfaces, and thereby two dimensional phase changes between gas-liquid-solid condensation and registry-disregistry transitions have also been studied.[2,3] The isotherms obtainable with these instruments are, however, restricted to the submonolayer regions only, since the scattering of electron beam by the gas molecules becomes increasingly significant with the increase in adsorbate gas pressure.The isotherms from submonolayer to multilayer regions are usually measured with a conventional volumetric or a gravimetric adsorption apparatus. The adsorbents in this case have to be prepared in the form of fine powder or porous state so as to provide at least a few square meters of surface area per gram of adsorbent. Accordingly, the adsorption results not only from the simple physisorption on the surfaces but also from the Kelvin condensation and the pendular ring condensation.

The idea of universal adsorption isotherm, namely the pure physisorption isotherm with no condensation contribution included in it, hypothetical in a sense, was proposed initially by Shull[4], and also by Cranston and Inkley[5] to evaluate the condensation contribution to the adsorption. A few more universal adsorption isotherms, based on empirical data, have been proposed thereafter.[6,7] The Frenkel-Halsey-Hill (FHH) equation[8], one of the improve BET equation, has been also accepted as an appropriate universal adsorption isotherm. Many other isotherms, derived on the basis of the model in which the adsorbent provides two dimensional homogeneous adsorption sites only, may also be used as universal adsorption isotherms, though not accepted generally. Ahn, one of the authors and Halsey have shown the appropriateness of the FHH equation as an universal adsorption isotherm in the previous paper of pore-size distribution analysis[9].

In this work, nitrogen adsorption isotherms on a number of adsorbents are measured using a gravimetric adsorption apparatus. The V-t plots, the plot of the volume adsorbed versus the statistical thickness of the adsorbed layer based on the universal adsorption isotherm, are made from these isotherms using various universal isotherms, and the resultant t-method areas are compared with the BET areas to see the appropriateness of universal isotherms.

Experimental

Material. Nitrogen gas, of purity 99.995% min., (from Daesung Sanso Co., Ltd., Korea) is used as the adsorbate. The adsorbents are obtained from diverse sources; Boron nitride powder of 325 mesh and purity 99% min. is from Alpha Products, Beverly Mass., U.S.A.: γ-alumina of purity 99.99% is from Kojundo Chemical Lab. Co., Ltd., Japan: Silica gel(A) of purity 99.9% is from Merck & Co., Inc., U.S.A.: And silica gel(B) was prepared as 325 mesh powder in this laboratory from reagent grade sodium silicate.

Apparatus. A gravimetric adsorption apparatus with the Nernst-Donau type quartz beam microbalance[10] is constructed. The schematic diagram is shown in Figure 1.
The system is pumped with a mechanical and a two stage oil diffusion pumps to the pressure of 10^{-6}mm. The pressure below 1mm is measured with a vacuum ionization gauge(GI-
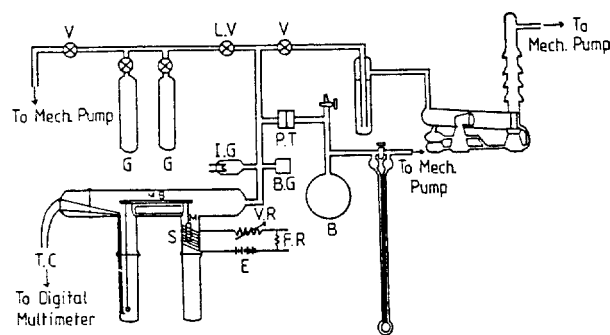

Figure 1. Schematic diagram of the adsorption apparatus. M.B: quartz beam microbalance, V.R: variable resistance, F.R: fixed resistance, V: Hoke valve, L.V: leak valve, I.G: ionization gauge, B.G: Baratron gauge, P.T: pressure transducer, M: magnet, S: solenoid, E: battery, B: ballast, G: gas, T.C: thermocouple

TL-2-Ulvac Corp., Japan) and a "Baratron" Capacitance type pressure transducer(310 CHS-1), and the pressure between 1mm and 760mm is measured with a mercury manometer. A pressure transducer(Model DP7, Validyne Engineering Corp., U.S.A) is used to bridge the mercury manometer and the sample chamber to avoid the mercury contamination of the sample chamber. The meniscus of the manometer is read off with a cathetometer.

The temperature of the system is kept at the liquid nitrogen temperature during the measurement by immersing the chamber arm in which the sample bucket is suspended. The temperature inside the arm near the bucket is monitored with copper-constantan thermocouple connected to a digital multimeter(177 microvolt DMM, Keithley Instruments Inc., U.S.A.).

Measurement. The sensitivity of the microbalance is determined in the vacuum by counterbalancing the loaded standard weight with the controlled electric current passing through the solenoid. Gold weights of known mass ranging from 372 μg through 3183 μg are used as standard weights. The linearity between the voltage consistent with the coun-

ter-balancing current and the mass of the standard weights was obtained with the correlation coefficient of 0.9998. The sensitivity was 2.05 μg/mV.

The buoyancy effect due to the volume difference between the two sides of the balance beam becomes significant as the pressure of the adsorbate gas increases. The volume difference is determined with an empty sample bucket as a function of the pressure at the liquid nitrogen temperature, and then it is extrapolated to zero pressure. The limitting volume difference obtained was 0.274cm^3, the bucket side being bulkier.

The system was heated to 250°C after the sample bucket was loaded with about 0.1g of adsorbent for about 12 hours in vacuum for degassing. After cooling, the chamber arm, inside of which the sample bucket was suspended, was immersed in liquid nitrogen. Then the adsorbate gas was introduced slowly through a variable leak valve (capable of controlling the inlet gas at the rate of 10^{-10}cc/sec through 100 cc/sec).

A considerable amount of heat is expected to be liberated by the gas adsorption whenever the adsorbate gas is intro-

Table 1. Physisorbed Amount of nitrogen on various Adsorbents at 77K

BN		γ-alumina		Silicagel(A)		Silicagel(B)	
P/P^o	V$_{ad}$(ml/g, STP)	P/P^o	V$_{ad}$(ml/g·STP)	P/P^o	V$_{ad}$(ml/g, STP)	P/P^o	V$_{ad}$(ml/g, STP)
0.0013	1.60	0.0014	23.12	0.0014	27.63	0.0013	6.98
0.0061	2.32	0.0113	33.42	0.0436	58.05	0.0375	12.85
0.0246	2.76	0.0239	35.51	0.0937	66.68	0.0640	15.53
0.0554	3.09	0.0357	37.61	0.1481	73.51	0.0948	15.58
0.0923	3.32	0.0526	40.24	0.2229	84.30	0.1243	17.46
0.1178	3.42	0.0642	41.53	0.2758	88.15	0.1544	18.22
0.1402	3.85	0.0752	42.81	0.3275	94.50	0.1813	19.37
0.1734	3.83	0.0867	44.17	0.3806	99.94	0.2150	20.36
0.2071	3.92	0.0975	45.24	0.4168	105.20	0.2485	21.68
0.2411	4.06	0.1156	47.00	0.4466	107.43	0.2868	22.94
0.2740	4.32	0.1360	49.00	0.4738	111.46	0.3192	23.67
0.3008	4.42	0.1594	50.99	0.5014	116.94	0.3660	25.05
0.3418	4.53	0.1850	53.30	0.5236	121.28	0.4145	26.45
0.3731	4.74	0.2106	55.37	0.5503	128.60	0.4626	27.89
0.3984	4.91	0.2375	57.59	0.5741	139.46	0.5034	29.20
0.4286	5.14	0.2634	59.40	0.6036	150.45	0.5475	30.59
0.4639	5.33	0.2875	61.24	0.6370	161.02	0.5877	31.81
0.5120	5.50	0.3251	63.54	0.6605	172.20	0.6314	33.25
0.5561	5.67	0.3539	65.83	0.6863	183.63	0.6779	35.29
0.5825	5.79	0.3822	67.64	0.7158	195.15	0.7145	36.82
		0.4111	69.43	0.7405	208.94	0.7721	39.83
		0.4377	70.78	0.7650	225.51	0.8190	42.36
		0.4834	73.38	0.7889	241.49	0.8696	46.74
		0.5110	75.36	0.8142	266.08	0.9242	53.58
		0.5432	76.80	0.8371	283.53	0.9825	64.55
		0.5803	79.00	0.8607	309.15		
		0.6191	81.04	0.8896	340.15		
		0.6548	83.57	0.9134	369.84		
		0.7226	86.88	0.9427	394.19		
		0.7529	89.33	0.9657	402.66		
		0.8036	92.19				
		0.8570	95.07				
		0.9083	98.91				
		0.9555	103.32				
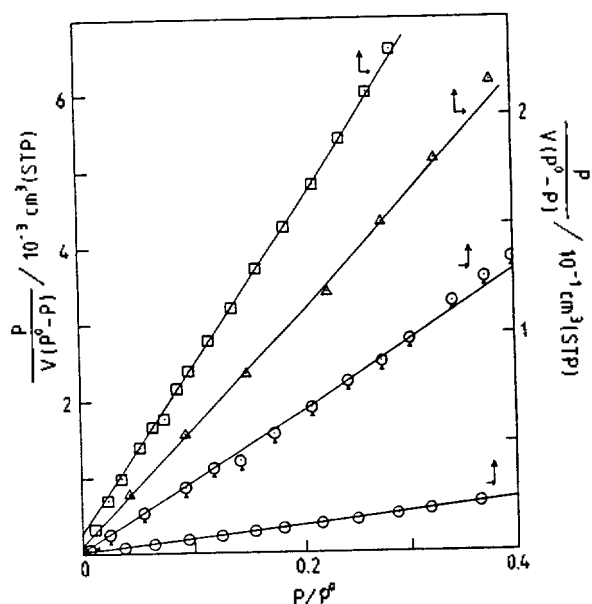
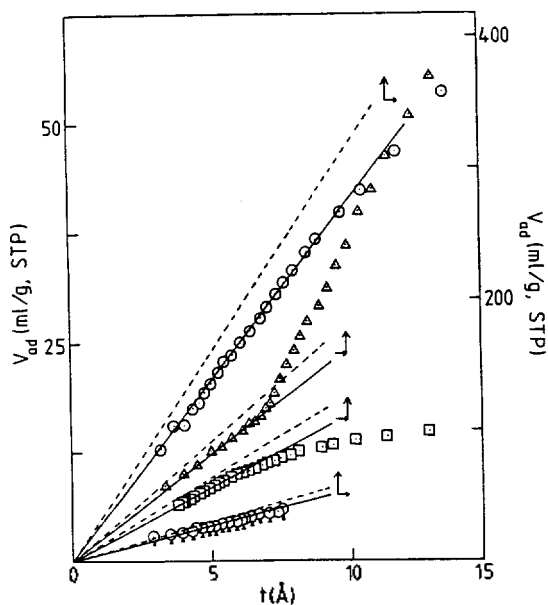**Figure 2.** BET plot. ♀, BN; ⊡, γ-alumina; △, Silicagel(A); ⊙, Silicagel(B).

Figure 4. The V-t plot based on Cranston & Inkley's universal adsorption isotherm. ♀, BN; ⊡, γ-alumina; △, Silicagel(A); ⊙, Silicagel(B).

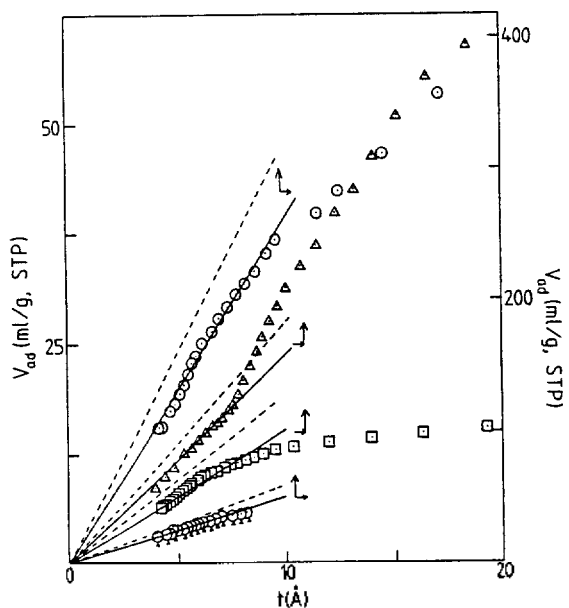**Figure 3.** The V-t plot based on Shull's universal adsorption isotherm. ♀, BN; ⊡, γ-alumina; △, Silicagel(A); ⊙, Silicagel(B).
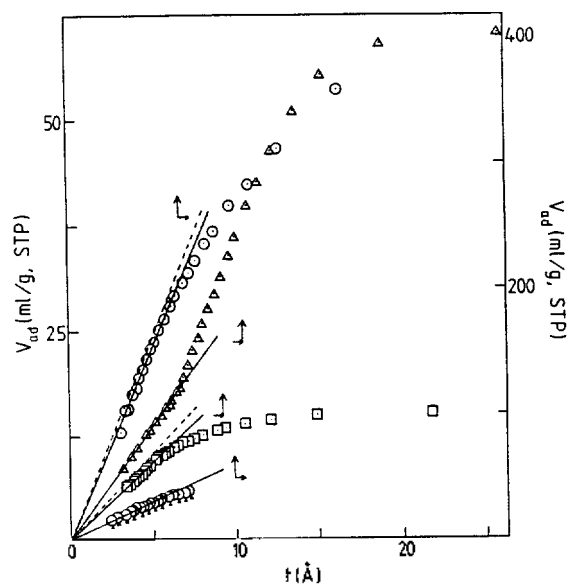
Figure 5. The V-t plot based on de Boer's universal adsorption isotherm. ♀, BN; ⊡, γ-alumina; △, Silicagel(A); ⊙, Silicagel(B).

duced into the system. The heat is expected to be transported away from the sample bucket with a limitted rate solely by the gas molecules. Therefore, a significant disturbance of the equilibrium temperature near the sample bucket is anticipated. In the experiment, it took at least an hour in restoring the equilibrium temperature. It took more than two hours, especially when the gas pressure was low and when the adsorbent has large surface area. The equilibrium temperature was measured with an accuracy of $\pm 4\mu V$ ($16\mu V$ correspond to 1 Kelvin) throughout the experiment.

Results and Discussion

The adsorption isotherms are measured on 4 different ad-

sorbents, and the data are given in Table 1. The amount of adsorbed gas is given in volume reduced to STP state per gram of adsorbent. All of the data are measured along the adsorption branch. The submonolayer region where two dimensional phase changes may occur is not investigated in this experiment. It is found that our gravimetric adsorption apparatus is unfavorable for this region, since it requires too long a time in restoring the equilibrium temperature. The isotherm with boron nitride is measured up to $p/p^{o} = 0.58$ only. Beyond this pressure, the counter-balancing current resulted mainly from the buoyancy effect, and the current due to the physisorption fell within the experimental error. The BET plots made from these isotherm data has yielded a fairly straight line in each case as shown in Figure 2. Two different

Table 2. Surface area of Adsorbents and adjusted Parameters of the FHH equation. The t-method area varies with the choice of universal Adsorption Isotherm

Adsorbent	BET area(m²/g)	t-method area (m²/g)					Parameters of the FHH equation	
		Shull	Cranston & Inkley	de Boer	Sing	FHH	s	b
BN	14	12	13	14	14	14	2.30	2.65
γ-alumina	199	157	175	191	198	200	2.00	2.29
Silicagel(A)	283	246	254	283	289	283	2.24	2.55
Silicagel(B)	74	61	64	71	76	74	1.83	2.17
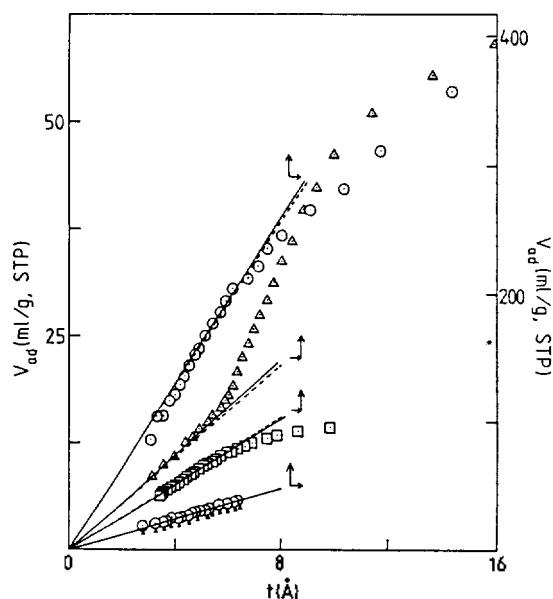
Figure 6. The V-t plot based on Sing's universal adsorption isotherm . ♀, BN; ⊡, γ-alumina; △, Silicagel(A); ○, Silicagel(B).
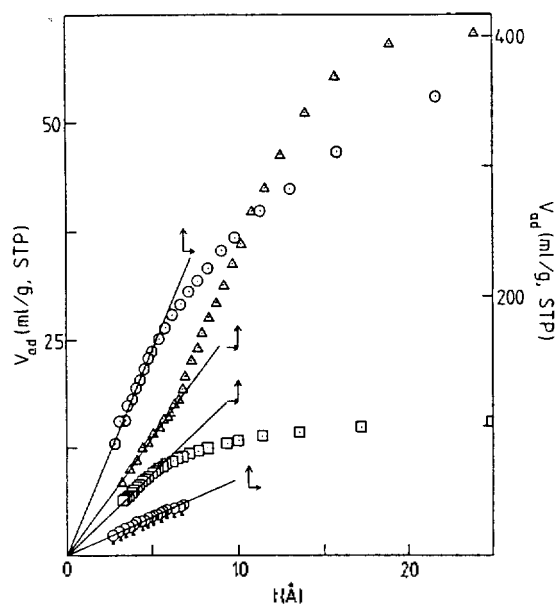
Figure 7. The V-t plot based on FHH's universal adsorption isotherm. ♀, BN; ⊡, γ-alumina; △, Silicagel(A); ○, Silicagel(B).

scales are used here for the ordinate to present all of the plots in a figure.

The V-t plots made with various universal adsorption isotherms are shown in Figure 3 through Figure 7. Two different scales are used for the ordinate in each of these figures.

The surface area of adsorbent can, also, be calculated from the slpe of the V-t plot in the lower t-region by the t-method.[11] The surface area calculated by this t-method are given in Table 2. The slope of the V-t plot deviates from the linearity when the surface area changes in the course of the adsorption.[9] The V-t plot which gives a negative deviation occurs when the surface area decreases without any Kelvin condensation during the adsorption. This deviation is observed when the adsorbent has slate-shaped pores. On the other hand, the positive deviation occurs when the adsorbent has pores, in which both the pure physisorption and the Kelvin condensation take place. This deviation is observed when the adsorbent has open-ended spherically cylindrical pores. Accordingly, hexagonal boron nitride is a non-porous adsorbent in the range of the measurement. More specifically, it has no pores, the radius of which is less than ca 24 Å. Silica gel have two types of pore structure, one(silica gel (A)) openended spherically cylindrical pores, and the other (silica gel (B)) slate-shaped pores.[12] The results of V-t plots in this work conform with these structures.

The broken lines in figures of the V-t plot are drawn to conform with the respective BET surface area. The slope of the V-t plot and the broken line coincide in Figure 7, where the FHH equation is used as an universal adsorption isotherm. The parameters of the FHH equation shown in Table 2 are fixed initially to give this coincidence. The V-t plots based on the Sing's isotherm give fairly good coincident slopes of the two lines. It is certain, however, that the universal adsorption isotherms cannot be judged with the degree of this coincidence alone. The results of pore size distribution analysis with various adsorbent should provide another basis for the judgement. The reason why the FHH equation is specifically considered in this work is that it is analytical and valid with other adsorbate gases as well as with nitrogen. Consequently, the equation might be used as the universal adsorption isotherm of other simple gases besides nitrogen.

References

1. R. A. Pierotti and H. E. Thomas in "Surface and Colloid Science", vol. IV, E. Matejevic, ed., Wiley-Interscience, New York, 1971, p 93.

2. S. C. Fain and M. D. Chinn, *J. Phys.(Paris), Colloq.*, **38**,

C4-99 (1977).

3. J. J. Lander and J. Morrison, *Surface Sci.*, **6**, 1 (1967).
4. C. G. Shull, *J. Amr. Chem. Soc.*, **70**, 1405 (1948).
5. R. W. Cranston and F. A. Inkley, *Adv. Catalysis*, **9**, 143 (1957).
6. J. H. de Boer, B. G. Linsen and Th. J. Osinga, *J. Catalysis*, **4**, 643 (1965).
7. S. J. Gregg and K. S. W. Sing, "Adsorption, Surface Area and Porosity", Academic Press, New York, 1982, p 41.
8. G. D. Halsey, *J. Chem. Phys.*, **16**, 931 (1948); *Adv. Cata-*

lysis, 263 (1952).

9. H. Cho, W. Ahn, and G. D. Halsey, *Bulletin of the Korea Chemical Society*, **1**, 94 (1988).
10. S. P. Wolsky and E. J. Zdanuk, "Ultra Micro Weight Determination in Controlled Environments", Interscience Publishers, 1969.
11. B. C. Lippens and J. H. de Boer, *J. Catalysis*, **4**, 319 (1965).
12. R. Sh. Mikhail, Stephen Brunauer, and E. E. Bodor, *J. Colloid and Interface Sci.*, **26**, 54 (1968).

Mechanism of Electropolymerization of Pyrrole in Acidic Aqueous Solutions

Kang-Jin Kim*, Hyung-Soo Song, and Jin-Doo Kim

Department of Chemistry, Korea University, Seoul 136-701

Jung-Kyoon Chon

Department of Chemistry, Han-Kuk University of Foreign Studies, Seoul 130-791
Received May 9, 1988

Mechanism of electrochemical polymerization of pyrrole (Py) on a Pt electrode in acidic aqueous solutions was studied by means of potentiostatic measurements, cyclic voltammetry and chronopotentiometry. Pyrrole molecule appeared to be initially oxidized via two-electron transfer step to produce oxidized pyrrole ion (Py^+), which was coupled with a non-oxidized pyrrole to yield a dimerized species, Py-Py. The Py-Py thus formed was further oxidized again via two-electron transfer step, which was followed by coupling with non-oxidized monomer and by concomitant expulsion of a H^+. Then the latter chain extension process was repeated. The chain extension and polypyrrole oxidation reactions occurred competitively.

Introduction

Recently interest in polypyrrole as a conducting polymer has been increasing rapidly.[1-4] Polypyrrole has received considerable interest because it can increase the stability of photoelectrodes used in converting solar energy to electrical or chemical energy.[5] However, there are only a few reports concerning with the detailed study on the mechanism of pyrrole polymerization under oxidizing conditions.[6-9]

Lundström and coworkers[6] suggested that the electropolymerization of pyrrole in the presence of fluoroborate (BF_4^-) ion was initiated by the oxidation of BF_4^-. Since the oxidation of BF_4^- does not occur until +3.0V, their suggestion is impossible to admit. Moreover, the electropolymerization of pyrrole on a Pt electrode could be achieved without BF_4^- in this study.

The literatures assume that the polymerization reaction is initiated by removal of one electron from pyrrole.[7-9] But the experimental data are insufficient to support this assumption. Diaz[7] proposes that the next step should involve the coupling of two radical cations on the ground that the concentration of the neutral aromatic species is zero at the electrode and negligible in the double layer region. Polymerization in solution was suggested similarly between cation radicals.[8] Considering the dimerization of small cation radicals being an unusual step, Pletcher *et al.* suggest that the dimer

should form between cation radical and neutral pyrrole with the expulsion of H^+ and two electrons.[9] Thus the mechanism of pyrrole electropolymerization is still not well understood.

Hence it is attempted to investigate the pyrrole polymerization process on a Pt electrode in acidic aqueous media for better understanding of the polymerization. To elucidate the electropolymerization in this study Tafel plots, cyclic voltammograms and chronopotentiograms were utilized.

Experimental

All chemicals, if not otherwise mentioned, were reagent grade and used without further purification. Pyrrole (Fluka AG, Purum) was vacuum distilled before use. All solutions were deoxigenated with a stream of nitrogen gas within an electrochemical cell before measurement. pH of solution was adjusted with either $H_3PO_4/H_2PO_4^-$ or $H_2PO_4^-/HPO_2^{2-}$ buffer solutions.

The electrochemical experiments were carried out in a three electrode system with a working electrode and a Pt gauze electrode separated by a Vycor frit and a S.C.E. reference electrode connected to the analyzing compartment through a Vycor frit. All the potentials given here are referred to S.C.E.. For most experiments, the working electrode was a Pt wire (area 0.19 cm^2) sealed into glass, which was freshly conditioned prior to each experiment.